Supplementary Information (SI) for Chemical Science.
This journal is © The Royal Society of Chemistry 2026

Supporting Information

Dimensional Engineering in Chiral Layered Hybrid Perovskites for High-Anisotropy Self-powered Circularly Polarized Light Detection

Wan Luo[a,b], *Qianxi Wang*[b], *Xiaoqi Li*[b], *Fen Zhang*[b], *Yan Fu*[a,b], *Yikun Fu*[a,b], *Xiaoyu Zhang*[a,b], *Guifu Zhang*[b], *Xitao Liu*[a,b,c*] and *Junhua Luo*[b,c]

[a]State Key Laboratory of Functional Crystals and Devices, Fujian Institute of Research on the Structure of Matter, Chinese Academy of Sciences Fuzhou, Fujian 350002, China.

[b]College of Chemistry and Materials Science, Fujian Normal University, Fuzhou, Fujian 350007, P.R. China University of Chinese Academy of Sciences, Beijing 100049, China.

[c]Fujian College, University of Chinese Academy of Sciences, Fuzhou, Fujian 350002, P.R. China.

Table of Contents

Table S1. Crystal data and structure refinement for $(R/S\text{-BrBA})_2EA_2Pb_3Br_{10}$ (3*R/S*).

Empirical formula	3*R*	3*S*
Formula weight	1818.95	1780.90
Temperature/K	293(2)	100.00(11)
Crystal system	monoclinic	monoclinic
Space group	$P2_1$	$P2_1$
a/Å	8.3135(3)	8.30260(10)
b/Å	8.4847(2)	8.46770(10)
c/Å	52.847(2)	52.7342(9)
α/°	90	90
β/°	90	90.071(2)
γ/°	90	90
Volume/Å^3	3727.7(2)	3707.42(9)
Z	4	4
ρ_{calc} g/cm^3	3.241	3.191
μ/mm^{-1}	26.391	26.532
$F(000)$	3216.0	3065.0
Crystal size/mm^3	0.3 × 0.2 × 0.1	0.3 × 0.2 × 0.1
Radiation	Mo Kα (λ = 0.71073)	Mo Kα (λ = 0.71073)
2Θ range for data collection/°	3.854 to 50.054	3.862 to 49.998
Index ranges	$-9 \le h \le 9$, $-10 \le k \le 10$, $-62 \le l \le 58$	$-9 \le h \le 9$, $-10 \le k \le 10$, $-59 \le l \le 62$
Reflections collected	33328	37739
Independent reflections	12549 [R_{int} = 0.0833, R_{sigma} = 0.0879]	12912 [R_{int} = 0.0483, R_{sigma} = 0.0541]
Data/restraints/parameters	12549/213/575	12912/420/575

Goodness-of-fit on F^2	1.063	1.047
Final R indexes [I>=2σ (I)	R_1 = 0.0818, wR_2 = 0.1798	R_1 = 0.0462, wR_2 = 0.1099
Final R indexes [all data]	R_1 = 0.0961, wR_2 = 0.1859	R_1 = 0.0581, wR_2 = 0.1156
Largest diff. peak/hole / e Å^{-3}	4.68/-5.16	2.82/-2.31
Flack parameter	0.003(14)	0.013(9)
CCDC number	2469041	2469438

Table S2. Atomic coordinates (x 10^4) and equivalent isotropic displacement parameters (Å^2 x 10^3) for 3*R*. *U*(eq) is defined as one third of the trace of the orthogonalized U_{ij} tensor.

Atoms	*x*	*y*	*z*	*U*(eq)
Pb1	6225(2)	2900(2)	2503.8(3)	15.3(4)
Pb2	11428(2)	7861(2)	1315.0(3)	11.9(4)
Pb3	11335.3(19)	7673(2)	3659.2(3)	11.7(4)
Pb4	6431.1(19)	2678.8(19)	3683.5(3)	10.1(4)
Pb5	6341(2)	2861(2)	1338.7(3)	12.4(4)
Br7	4373(6)	6037(6)	2503.1(10)	19.3(11)
Br8	3172(6)	707(6)	2494.2(9)	16.5(10)
Br9	8165(6)	-166(6)	2503.7(9)	15.6(10)
Br10	9183(6)	4750(6)	3785.5(10)	18.7(11)
Br11	11406(8)	7923(8)	1937.4(10)	35.7(15)
Br12	9386(6)	4503(6)	2497.4(10)	18.5(11)
Br13	11570(7)	7952(8)	3058.0(12)	37.6(14)
Br14	6210(6)	1956(6)	4202.9(9)	17.9(11)
Br15	9039(6)	5187(6)	1200.7(10)	17.8(11)
Br16	11217(7)	8581(6)	795.7(10)	22.5(12)
Br17	10666(5)	8461(5)	4171.4(9)	13.3(10)
Br18	14178(6)	5766(6)	1216.5(10)	21.6(12)
Br20	5673(6)	2084(6)	826.9(9)	15.3(10)
Br24	13770(6)	10135(6)	3655.0(10)	19.7(11)
Br25	6400(9)	2627(8)	3062.0(10)	36.2(15)
Br27	13668(6)	10521(6)	1424.0(10)	20.8(12)
Br28	6558(8)	2589(9)	1941.6(13)	40.8(15)
Br29	14028(6)	5365(6)	3796.8(10)	16.1(11)
Pb6	11223(2)	7637(2)	2495.4(3)	14.8(4)
Br1	8783(6)	408(6)	1340.0(10)	20.1(12)
Br4	8658(6)	18(6)	3574.7(10)	18.8(11)
Br2	5093(7)	9101(7)	4917.3(10)	27.6(12)

Br3	10090(7)	1437(7)	82.9(11)	32.3(13)
Br5	8940(7)	1381(10)	4850.7(11)	44.3(17)
Br6	3949(8)	9144(11)	147.5(12)	53(2)
C1	6230(60)	7760(60)	622(10)	24(11)
C2	11270(50)	2770(50)	4386(8)	8(8)
N3	11700(40)	2550(40)	917(7)	13(8)
C6	6440(60)	7710(60)	4359(10)	24(11)
C16	4050(50)	7720(50)	4675(8)	13(9)
C19	11770(70)	4480(60)	4437(11)	26(12)
C20	9050(60)	2860(60)	326(10)	28(11)
C21	4590(60)	8010(60)	4391(10)	21(10)
C23	9620(60)	2530(60)	606(10)	27(11)
C26	6280(60)	8650(60)	151(10)	19(10)
C31	11250(70)	1890(70)	4858(12)	33(13)
C39	11950(50)	1710(50)	4582(9)	14(9)
C57	6920(60)	8840(60)	417(11)	27(11)
N5	6730(40)	8030(40)	4086(7)	10(8)
N9	11900(50)	2350(50)	4124(8)	22(9)
C12	11440(70)	2840(70)	623(11)	31(12)
N37	6870(60)	8210(50)	873(9)	32(11)
C44	7040(70)	6120(60)	4433(11)	29(13)
C66	6710(60)	6110(60)	562(11)	25(12)
C8	10280(70)	1860(60)	2992(11)	30(13)
C17	10740(90)	3040(90)	3189(14)	66(19)
C22	10460(50)	1870(40)	2010(8)	4(8)
N1	12330(100)	3470(110)	1892(18)	100(30)
N36	12270(100)	3700(120)	3119(19)	120(30)
N15	5290(60)	8780(60)	2001(10)	35(12)
C81	7090(120)	6560(90)	1870(20)	80(30)
C97	6660(100)	8220(90)	1850(18)	90(20)
N4	5470(50)	8670(40)	2998(8)	16(8)
C40	5780(120)	7360(110)	3186(18)	110(30)

C45	12050(60)	4430(60)	562(11)	24(12)
C89	7420(110)	6910(120)	3100(20)	110(40)
C35	10750(90)	3270(90)	1827(16)	59(18)

Table S3. Atomic coordinates (x 10^4) and equivalent isotropic displacement parameters (Å^2 x 10^3) for 3*S*. *U*(eq) is defined as one third of the trace of the orthogonalized U_{ij} tensor.

Atom	*z*	*y*	*z*	*U*(eq)
Pb1	3571.3(11)	-2433(5)	1316.8(2)	15.7(2)
Pb2	-1343.6(10)	2566(5)	1339.9(2)	15.9(2)
Pb3	-1231.4(11)	2619(5)	2504.3(2)	18.9(2)
Pb4	3767.2(11)	7356(5)	2496.9(2)	19.0(2)
Pb5	3653.5(10)	7408(5)	3661.6(2)	16.1(2)
Pb6	8572.9(11)	12406(5)	3684.2(2)	15.8(2)
Br1	5963(3)	-5113(6)	1203.1(5)	23.7(6)
Br2	826(3)	-4517(6)	1215.9(5)	28.0(7)
Br3	3790(4)	-1715(6)	797.5(5)	27.5(6)
Br4	1339(3)	228(6)	1423.9(5)	26.3(7)
Br5	-684(3)	1801(6)	827.2(5)	22.1(6)
Br6	-3772(3)	114(6)	1343.4(5)	24.9(6)
Br7	-1561(4)	2297(7)	1941.1(5)	43.2(9)
Br8	-3171(3)	-451(6)	2503.9(5)	20.6(6)
Br9	-1406(4)	2352(7)	3062.5(5)	41.3(8)
Br10	-4382(3)	4221(6)	2500.3(5)	21.3(6)
Br11	617(3)	5750(6)	2500.9(5)	21.2(6)
Br12	3588(4)	7633(7)	1937.8(5)	39.3(8)
Br13	1826(3)	10415(6)	2497.3(5)	20.5(6)
Br14	3438(4)	7683(7)	3060.0(5)	43.1(9)
Br15	4312(3)	8176(6)	4175.0(5)	23.2(6)
Br16	1223(3)	9864(6)	3658.7(5)	25.2(6)
Br17	6333(3)	9744(6)	3577.7(6)	28.9(7)

Atom	*z*	*y*	*z*	*U*(eq)
Br18	8781(4)	11690(6)	4203.1(5)	30.5(7)
Br19	5828(4)	14496(6)	3784.0(5)	29.5(7)
Br20	10965(3)	15085(6)	3797.8(5)	24.2(6)
Br21	1058(4)	8850(8)	148.7(7)	62.9(12)
N1	-1880(30)	7970(20)	867(2)	29(3)
C1	-1255(14)	8400(20)	156(2)	30(3)
C2	-1928(15)	8565(17)	415(2)	30(3)
C3	-1253(19)	7454(16)	615(2)	30(3)
C16	-1730(30)	5757(14)	566(3)	30(3)
Br22	4903(4)	1144(6)	82.0(5)	39.3(8)
N2	3300(19)	2240(20)	918(2)	24(3)
C20	5909(18)	2578(19)	327(2)	25(3)
C19	5360(15)	2250(20)	590(2)	24(3)
C5	3576(16)	2483(17)	641(2)	24(3)
C22	3010(20)	4114(19)	564(3)	25(3)
Br23	-95(4)	8827(6)	4918.8(6)	40.9(8)
N3	-1718(19)	7760(20)	4084(2)	25(3)
C9	927(18)	7420(20)	4673(2)	26(3)
C10	363(16)	7740(20)	4410(2)	26(3)
C11	-1421(16)	7488(17)	4361(2)	26(3)
C12	-1960(20)	5840(19)	4433(4)	26(3)
Br24	6057(4)	1125(8)	4851.1(7)	66.4(12)
C4	3220(30)	4183(15)	4442(4)	36(3)
C13	3759(15)	1650(30)	4849(3)	35(3)
C14	3045(15)	1470(17)	4592(2)	35(3)
C15	3735(19)	2527(17)	4386(2)	35(3)
N16	3150(30)	2050(20)	4125(2)	35(3)
N5	-330(30)	8510(30)	2007(5)	63(6)
C17	-1700(30)	7960(20)	1849(6)	65(6)
C18	-1760(40)	6270(20)	1870(7)	65(6)

Atom	*z*	*y*	*z*	*U*(eq)
N6	-440(30)	8430(30)	2992(5)	50(5)
C7	4610(30)	1530(30)	2010(5)	41(4)
C21	4160(20)	2870(30)	1844(5)	43(4)
N22	2510(20)	3250(30)	1896(5)	45(4)
C8	4670(30)	1480(30)	2989(5)	61(6)
C23	4200(30)	2730(40)	3172(5)	62(6)
N24	2540(20)	3090(30)	3126(5)	63(6)
C19A	-2400(40)	6510(40)	3096(6)	53(5)
C20A	-770(40)	7030(40)	3162(6)	52(5)

Table S4. Selected bond lengths (Å) for 3*R*.

Atom-Atom	Length（(Å)	Atom-Atom	Length(Å)
Pb1-Br7	3.075(5)	Br9-Pb6[4]	3.153(5)
Pb1-Br8	3.148(5)	Br11-Pb6	2.963(6)
Pb1-Br9	3.061(5)	Br12-Pb6	3.067(5)
Pb1-Br12	2.959(5)	Br13-Pb6	2.999(6)
Pb1-Br25	2.962(5)	Br2-C16	1.94(4)
Pb1-Br28	2.996(7)	Br3-C20	1.96(6)
Pb2-Br11	3.290(6)	Br5-C31	1.97(6)
Pb2-Br15	3.076(5)	Br6-C26	1.98(5)
Pb2-Br16	2.817(5)	C1-C57	1.53(8)
Pb2-Br18	2.942(5)	C1-N37	1.48(7)
Pb2-Br27	2.982(5)	C1-C66	1.49(7)
Pb2-Br11	3.086(5)	C2-C19	1.53(7)
Pb3-Br10	3.131(5)	C2-C39	1.48(6)
Pb3-Br13	3.192(7)	C2-N9	1.52(6)
Pb3-Br17	2.843(5)	N3-C12	1.59(7)
Pb3-Br24	2.909(5)	C6-C21	1.57(7)
Pb3-Br29	3.062(5)	C6-N5	1.49(6)
Pb3-Br4[1]	3.019(5)	C6-C44	1.49(7)
Pb4-Br10	2.934(5)	C16-C21	1.59(7)
Pb4-Br14	2.818(5)	C20-C23	1.58(7)

Pb4-Br24[2]	3.094(5)	C23-C12	1.54(7)
Pb4-Br25	3.285(5)	C26-C57	1.51(7)
Pb4-Br29[3]	3.089(5)	C31-C39	1.58(8)
Pb4-Br4	2.976(5)	C12-C45	1.47(8)
Pb5-Br15	3.075(5)	C8-C17	1.49(5)
Pb5-Br18[3]	3.119(5)	C17-N36	1.44(5)
Pb5-Br20	2.839(5)	C22-C35	1.55(9)
Pb5-Br27[2]	3.015(5)	N1-C35	1.37(10)
Pb5-Br28	3.199(7)	N15-C97	1.47(5)
Pb5-Br1	2.907(5)	C81-C97	1.46(5)
Br7-Pb6[3]	2.950(5)	N4-C40	1.51(3)
Br8-Pb6[2]	3.067(5)	C40-C89	1.49(3)

[1]+X,1+Y,+Z; [2]-1+X,-1+Y,+Z; [3]-1+X,+Y,+Z; [4]+X,-1+Y,+Z; [5]1+X,+Y,+Z; [6]1+X,1+Y,+Z

Table S5. Selected bond lengths (Å) for 3*S*.

Atom-Atom	Length (Å)	Atom-Atom	Length (Å)
Pb1-Br1	3.076(3)	Pb6-Br18	2.808(3)
Pb1-Br2	2.931(3)	Pb6-Br19	2.934(3)
Pb1-Br3	2.811(3)	Pb6-Br20	3.074(3)
Pb1-Br4	2.972(3)	Br21-C1	1.959(11)
Pb1-Br6[1]	3.088(3)	N1-C3	1.494(13)
Pb1-Br12[2]	3.275(3)	C1-C2	1.486(13)
Pb2-Br1[3]	3.062(3)	C2-C3	1.519(14)
Pb2-Br24	3.127(3)	C3-C16	1.513(14)
Pb2-Br4	3.012(3)	Br22-C20	1.959(11)
Pb2-Br5	2.834(3)	N2-C5	1.494(13)
Pb2-Br6	2.894(3)	C20-C19	1.486(13)
Pb2-Br7	3.184(3)	C19-C5	1.519(14)
Pb3-Br7	2.995(3)	C5-C22	1.513(14)
Pb3-Br8	3.057(3)	Br23-C9	1.959(11)
Pb3-Br9	2.956(3)	N3-C11	1.494(13)
Pb3-Br10	2.947(3)	C9-C10	1.486(13)
Pb3-Br11	3.063(3)	C10-C11	1.519(14)
Pb3-Br13[2]	3.151(3)	C11-C12	1.513(14)

Pb4-Br8^{5}	3.149(3)	Br24-C13	1.959(11)
Pb4-Br10^{1}	3.067(3)	C4-C15	1.494(13)
Pb4-Br11	2.948(3)	C13-C14	1.486(13)
Pb4-Br12	2.961(3)	C14-C15	1.519(14)
Pb4-Br13	3.051(3)	C15-N16	1.514(14)
Pb4-Br14	2.995(3)	N5-C17	1.485(13)
Pb5-Br14	3.186(3)	C17-C18	1.433(13)
Pb5-Br15	2.837(3)	N6-C20A	1.508(18)
Pb5-Br16	2.898(3)	C7-C21	1.485(13)
Pb5-Br17	3.010(3)	C21-N22	1.433(13)
Pb5-Br19^{2}	3.123(3)	C8-C23	1.485(13)
Pb5-Br20^{6}	3.061(3)	C23-N24	1.433(13)
Pb6-Br16^{1}	3.081(3)	C19A-C20A	1.463(19)
Pb6-Br17	2.975(3)		

^{1}1+X,+Y,+Z; ^{2}+X,-1+Y,+Z; ^{3}-1+X,1+Y,+Z; ^{4}+X,1+Y,+Z; ^{5}1+X,1+Y,+Z; ^{6}-1+X,-1+Y,+Z

Table S6. Selected bond angles (°) for 3*R*.

Atom-Atom-Atom	Angle(°)	Atom-Atom-Atom	Angle(°)
Br7-Pb1-Br8	96.21(14)	Br20-Pb5-Br27^{2}	81.09(15)
Br9-Pb1-Br7	178.26(16)	Br20-Pb5-Br28	160.55(18)
Br9-Pb1-Br8	85.53(16)	Br20-Pb5-Br1	88.43(15)
Br12-Pb1-Br7	92.69(17)	Br27^{2}-Pb5-Br15	174.86(15)
Br12-Pb1-Br8	170.96(16)	Br27^{2}-Pb5-Br18^{3}	97.26(15)
Br12-Pb1-Br9	85.57(14)	Br27^{2}-Pb5-Br28	81.08(16)
Br12-Pb1-Br25	90.22(18)	Br1-Pb5-Br15	87.18(15)
Br12-Pb1-Br28	86.96(17)	Br1-Pb5-Br18^{3}	165.67(17)
Br25-Pb1-Br7	95.37(17)	Br1-Pb5-Br27^{2}	92.45(17)
Br25-Pb1-Br8	90.54(17)	Br1-Pb5-Br28	84.64(17)
Br25-Pb1-Br9	84.71(16)	Pb6^{3}-Br7-Pb1	147.4(2)
Br25-Pb1-Br28	167.4(2)	Pb6^{2}-Br8-Pb1	158.13(18)
Br28-Pb1-Br7	96.98(17)	Pb1-Br9-Pb6^{4}	158.01(18)
Br28-Pb1-Br8	90.36(17)	Pb4-Br10-Pb3	151.75(18)
Br28-Pb1-Br9	82.88(17)	Pb6-Br11-Pb2	173.8(2)
Br15-Pb2-Br11	101.80(16)	Pb1-Br12-Pb6	147.2(2)

Br15-Pb2-Br1^{1}	93.71(14)	Pb6-Br13-Pb3	167.0(2)
Br16-Pb2-Br11	166.01(17)	Pb5-Br15-Pb2	153.88(19)
Br16-Pb2-Br15	85.88(15)	Pb2-Br18-Pb5^{5}	152.7(2)
Br16-Pb2-Br18	90.41(16)	Pb3-Br24-Pb4^{6}	176.4(2)
Br16-Pb2-Br27	93.63(16)	Pb1-Br25-Pb4	174.2(2)
Br16-Pb2-Br1^{1}	81.12(16)	Pb2-Br27-Pb5^{6}	158.4(2)
Br18-Pb2-Br11	100.98(17)	Pb1-Br28-Pb5	167.4(3)
Br18-Pb2-Br15	91.23(15)	Pb3-Br29-Pb4^{5}	153.96(18)
Br18-Pb2-Br27	90.35(16)	Br7^{5}-Pb6-Br8^{6}	85.52(14)
Br18-Pb2-Br1^{1}	169.85(17)	Br7^{5}-Pb6-Br9^{1}	171.03(15)
Br27-Pb2-Br11	78.35(16)	Br7^{5}-Pb6-Br11	90.33(18)
Br27-Pb2-Br15	178.35(15)	Br7^{5}-Pb6-Br12	92.46(17)
Br27-Pb2-Br1^{1}	84.65(16)	Br7^{5}-Pb6-Br13	86.68(17)
Br1^{1}-Pb2-Br11	86.68(17)	Br8^{6}-Pb6-Br9^{1}	85.66(16)
Br10-Pb3-Br13	107.82(16)	Br11-Pb6-Br8^{6}	84.34(16)
Br17-Pb3-Br10	82.61(14)	Br11-Pb6-Br9^{1}	90.40(17)
Br17-Pb3-Br13	160.40(17)	Br11-Pb6-Br12	95.74(16)
Br17-Pb3-Br24	88.54(15)	Br11-Pb6-Br13	167.0(2)
Br17-Pb3-Br29	93.87(14)	Br12-Pb6-Br8^{6}	177.98(15)
Br17-Pb3-Br4^{1}	80.88(14)	Br12-Pb6-Br9^{1}	96.36(14)
Br24-Pb3-Br10	165.55(15)	Br13-Pb6-Br8^{6}	82.85(16)
Br24-Pb3-Br13	84.06(16)	Br13-Pb6-Br9^{1}	90.63(16)
Br24-Pb3-Br29	87.26(15)	Br13-Pb6-Br12	96.99(17)
Br24-Pb3-Br4^{1}	92.22(17)	Pb5-Br1-Pb2^{4}	177.1(2)
Br29-Pb3-Br10	81.99(14)	Pb4-Br4-Pb3^{4}	158.46(19)
Br29-Pb3-Br13	103.85(16)	N37-C1-C57	110(4)
Br4^{1}-Pb3-Br10	97.59(15)	N37-C1-C66	110(4)
Br4^{1}-Pb3-Br13	81.31(16)	C66-C1-C57	108(5)
Br4^{1}-Pb3-Br29	174.73(15)	C39-C2-C19	111(4)
Br10-Pb4-Br24^{2}	169.71(15)	C39-C2-N9	111(4)
Br10-Pb4-Br25	101.41(17)	N9-C2-C19	107(4)
Br10-Pb4-Br29^{3}	91.53(14)	N5-C6-C21	103(4)
Br10-Pb4-Br4	90.28(15)	N5-C6-C44	111(5)
Br14-Pb4-Br10	90.13(15)	C44-C6-C21	116(5)

Br14-Pb4-Br24^{2}	81.32(15)	C21-C16-Br2	114(3)
Br14-Pb4-Br25	166.01(16)	C23-C20-Br3	112(4)
Br14-Pb4-Br29^{3}	85.96(15)	C6-C21-C16	111(4)
Br14-Pb4-Br4	93.66(15)	C12-C23-C20	109(5)
Br24^{2}-Pb4-Br25	86.35(17)	C57-C26-Br6	109(4)
Br29^{3}-Pb4-Br24^{2}	93.55(14)	C39-C31-Br5	108(3)
Br29^{3}-Pb4-Br25	101.45(15)	C2-C39-C31	117(4)
Br4-Pb4-Br24^{2}	84.61(16)	C26-C57-C1	118(4)
Br4-Pb4-Br25	78.55(15)	C23-C12-N3	99(4)
Br4-Pb4-Br29^{3}	178.15(15)	C45-C12-N3	108(4)
Br15-Pb5-Br18^{3}	82.20(15)	C45-C12-C23	119(5)
Br15-Pb5-Br28	103.98(16)	N36-C17-C8	108(7)
Br18^{3}-Pb5-Br28	107.21(17)	N15-C97-C81	118(7)
Br20-Pb5-Br15	93.78(15)	C89-C40-N4	98(4)
Br20-Pb5-Br18^{3}	82.73(14)	N1-C35-C22	95(6)

^{1}+X,1+Y,+Z; ^{2}-1+X,-1+Y,+Z; ^{3}-1+X,+Y,+Z; ^{4}+X,-1+Y,+Z; ^{5}1+X,+Y,+Z; ^{6}1+X,1+Y,+Z

Table S7. Selected bond angles (°) for 3*S*.

Atom-Atom-Atom	Angle(°)	Atom-Atom-Atom	Angle(°)
Br1-Pb1-Br6^{1}	93.61(8)	Br15-Pb5-Br17	81.25(8)
Br1-Pb1-Br12^{2}	101.85(9)	Br15-Pb5-Br19^{2}	82.70(8)
Br2-Pb1-Br1	91.28(9)	Br15-Pb5-Br20^{6}	93.61(8)
Br2-Pb1-Br4	90.33(9)	Br16-Pb5-Br14	84.50(9)
Br2-Pb1-Br6^{1}	169.78(9)	Br16-Pb5-Br17	92.42(10)
Br2-Pb1-Br12^{2}	101.19(9)	Br16-Pb5-Br19^{2}	165.96(9)
Br3-Pb1-Br1	85.83(8)	Br16-Pb5-Br20^{6}	87.38(8)
Br3-Pb1-Br2	90.26(9)	Br17-Pb5-Br14	81.16(9)
Br3-Pb1-Br4	93.57(9)	Br17-Pb5-Br19^{2}	97.01(9)
Br3-Pb1-Br6^{1}	81.16(8)	Br17-Pb5-Br20^{6}	174.87(8)
Br3-Pb1-Br12^{2}	165.96(10)	Br19^{2}-Pb5-Br14	107.18(9)
Br4-Pb1-Br1	178.28(9)	Br20^{6}-Pb5-Br14	103.92(9)
Br4-Pb1-Br6^{1}	84.70(9)	Br20^{6}-Pb5-Br19^{2}	82.29(8)
Br4-Pb1-Br12^{2}	78.41(9)	Br17-Pb6-Br16^{1}	84.77(9)

Br6^{1}-Pb1-Br12^{2}	86.59(9)	Br17-Pb6-Br20	178.33(9)
Br13-Pb2-Br2^{4}	82.21(8)	Br18-Pb6-Br16^{1}	81.30(9)
Br1^{3}-Pb2-Br7	103.79(9)	Br18-Pb6-Br17	93.34(9)
Br2^{4}-Pb2-Br7	107.35(9)	Br18-Pb6-Br19	90.13(9)
Br4-Pb2-Br1^{3}	174.82(8)	Br18-Pb6-Br20	86.00(9)
Br4-Pb2-Br2^{4}	97.13(8)	Br19-Pb6-Br16^{1}	169.84(9)
Br4-Pb2-Br7	81.33(9)	Br19-Pb6-Br17	90.31(9)
Br5-Pb2-Br1^{3}	93.65(8)	Br19-Pb6-Br20	91.23(9)
Br5-Pb2-Br2^{4}	82.47(8)	Br20-Pb6-Br16^{1}	93.61(8)
Br5-Pb2-Br4	81.17(8)	Pb2^{7}-Br1-Pb1	154.04(10)
Br5-Pb2-Br6	88.72(8)	Pb1-Br2-Pb2^{2}	152.35(11)
Br5-Pb2-Br7	160.87(10)	Pb1-Br4-Pb2	158.66(11)
Br6-Pb2-Br1^{3}	87.33(8)	Pb2-Br6-Pb1^{8}	176.67(12)
Br6-Pb2-Br2^{4}	165.83(9)	Pb3-Br7-Pb2	167.38(15)
Br6-Pb2-Br4	92.43(9)	Pb3-Br8-Pb4^{6}	157.93(10)
Br6-Pb2-Br7	84.37(9)	Pb3-Br9-Pb6^{6}	174.26(14)
Br7-Pb3-Br8	82.80(10)	Pb3-Br10-Pb4^{8}	147.49(11)
Br7-Pb3-Br11	96.78(10)	Pb4-Br11-Pb3	147.53(11)
Br7-Pb3-Br13^{2}	90.40(9)	Pb4-Br13-Pb3^{4}	158.19(10)
Br8-Pb3-Br11	178.24(8)	Pb4-Br14-Pb5	167.28(15)
Br8-Pb3-Br13^{2}	85.47(9)	Pb5-Br16-Pb6^{8}	176.81(11)
Br9-Pb3-Br7	167.46(12)	Pb6-Br17-Pb5	158.77(12)
Br9-Pb3-Br8	84.80(9)	Pb6-Br19-Pb5^{4}	152.66(11)
Br9-Pb3-Br11	95.57(9)	Pb5^{5}-Br20-Pb6	154.11(10)
Br9-Pb3-Br13^{2}	90.41(9)	C2-C1-Br21	111.6(8)
Br10-Pb3-Br7	87.41(9)	C1-C2-C3	116.1(8)
Br10-Pb3-Br8	85.64(8)	N1-C3-C2	107.8(8)
Br10-Pb3-Br9	89.87(9)	N1-C3-C16	109.8(9)
Br10-Pb3-Br11	92.64(9)	C16-C3-C2	111.9(9)
Br10-Pb3-Br13^{2}	171.04(9)	C19-C20-Br22	111.6(8)
Br11-Pb3-Br13^{2}	96.25(7)	C20-C19-C5	116.1(8)
Br10^{1}-Pb4-Br8^{5}	96.09(7)	N2-C5-C19	107.8(8)
Br11-Pb4-Br8^{5}	171.25(9)	N2-C5-C22	109.8(9)
Br11-Pb4-Br10^{1}	92.59(9)	C22-C5-C19	111.9(9)

Br11-Pb4-Br12	90.02(9)	C10-C9-Br23	111.6(8)
Br11-Pb4-Br13	85.59(8)	C9-C10-C11	116.1(8)
Br11-Pb4-Br14	87.34(9)	N3-C11-C10	107.8(8)
Br12-Pb4-Br8[5]	90.26(9)	N3-C11-C12	109.8(9)
Br12-Pb4-Br10[1]	95.67(9)	C12-C11-C10	111.9(9)
Br12-Pb4-Br13	84.70(9)	C14-C13-Br24	111.6(8)
Br12-Pb4-Br14	167.23(12)	C13-C14-C15	116.1(8)
Br13-Pb4-Br8[5]	85.73(9)	C4-C15-C14	107.8(8)
Br13-Pb4-Br10[1]	178.15(8)	C4-C15-N16	109.8(9)
Br14-Pb4-Br8[5]	90.48(9)	N16-C15-C14	111.9(9)
Br14-Pb4-Br10[1]	96.92(10)	C18-C17-N5	107.2(13)
Br14-Pb4-Br13	82.65(10)	N22-C21-C7	107.2(13)
Br15-Pb5-Br14	160.75(11)	N24-C23-C8	107.2(13)
Br15-Pb5-Br16	88.50(8)	C19A-C20A-N6	105(2)

[1] 1+X,+Y,+Z; [2] +X,-1+Y,+Z; [3] -1+X,1+Y,+Z; [4] +X,1+Y,+Z; [5] 1+X,1+Y,+Z; [6] -1+X,-1+Y,+Z; [7] 1+X,-1+Y,+Z; [8] -1+X,+Y,+Z

Table S8. Crystal data and structure refinement for (*R/S*-BrBA)$_2$EAPb$_2$Br$_7$ (2*R/S*).

Empirical formula	2*R*	2*S*
Formula weight	1325.94	1325.94
Temperature/K	100.15	293(2)
Crystal system	orthorhombic	orthorhombic
Space group	$P2_12_12_1$	$P2_12_12_1$
a/Å	8.1959(2)	8.40870(10)
b/Å	8.6590(2)	8.59910(10)
c/Å	40.5557(10)	40.7961(3)
α/°	90	90
β/°	90	90
γ/°	90	90
Volume/Å^3	2878.17(12)	2949.85(5)
Z	4	4
ρ_{calc} g/cm^3	3.060	2.986
μ/mm^{-1}	24.830	36.237
F(000)	2360.0	2360.0

Crystal size/mm^3	0.3 × 0.2 × 0.1	0.3 × 0.2 × 0.1
Radiation	Ga Kα (λ = 1.3405)	Cu Kα (λ = 1.54184)
2Θ range for data collection/°	3.788 to 112.13	4.332 to 133.176
Index ranges	$-10 \leq h \leq 10$, $-10 \leq k \leq 10$, $-49 \leq l \leq 49$	$-10 \leq h \leq 10$, $-10 \leq k \leq 8$, $-48 \leq l \leq 48$
Reflections collected	102640	53371
Independent reflections	5537 [Rint = 0.0946, Rsigma = 0.0271]	5207 [Rint = 0.1110, Rsigma = 0.0374]
Data/restraints/parameters	5537/0/223	5207/38/223
Goodness-of-fit on F^2	1.121	1.039
Final R indexes [I>=2σ (I)]	R_1 = 0.0318, wR_2 = 0.0811	R_1 = 0.0501, wR_2 = 0.1477
Final R indexes [all data]	R_1 = 0.0324, wR_2 = 0.0822	R_1 = 0.0525, wR_2 = 0.1510
Largest diff. peak/hole / e Å^{-3}	2.09/-3.63	2.34/-2.00
Flack parameter	-0.001(4)	-0.036(7)
CCDC number	2520919	2520920

Table S9. Fractional Atomic Coordinates (× 10^4) and Equivalent Isotropic Displacement Parameters (Å^2 × 10^3) for 2*R*. U_{eq} is defined as 1/3 of the trace of the orthogonalised U_{IJ} tensor.

Atom	*x*	*y*	*z*	*U*(eq)
Pb01	7214.5(5)	10777.2(5)	6756.4(2)	9.78(12)
Pb02	2234.2(5)	5827.1(5)	6719.0(2)	8.95(12)
Br03	1922.9(14)	6457.8(15)	6000.9(3)	13.1(2)
Br04	7880.7(15)	10464.9(15)	6079.0(3)	14.6(2)
Br05	119.3(14)	8542.4(15)	6825.7(3)	14.2(3)
Br06	5097.9(15)	8032.0(15)	6675.8(3)	16.5(3)
Br07	4176.9(14)	12685.3(15)	6675.3(3)	16.1(3)
Br08	2282.4(16)	5535.5(16)	7459.5(3)	15.1(3)
Br09	-629.0(15)	3703.8(16)	6699.4(3)	18.6(3)

Atom	*x*	*y*	*z*	*U*(eq)
Br0A	6343.2(18)	7464(2)	4877.9(3)	27.7(3)
Br0B	-263(2)	12318(2)	5215.5(4)	44.2(5)
N00C	7888(13)	6607(13)	6140(2)	17(2)
N00D	1581(14)	1813(13)	7347(3)	21(2)
C00E	3783(15)	10336(16)	5669(3)	21(3)
N00F	2027(12)	10252(13)	6157(2)	16(2)
C00G	5824(16)	6488(17)	5297(3)	21(3)
C00H	3220(17)	-415(16)	7542(3)	21(3)
C00I	7125(15)	6811(15)	5551(3)	18(3)
C00J	2125(14)	10781(14)	5804(3)	14(2)
C00K	6643(15)	6099(15)	5886(3)	15(2)
C00L	1743(15)	12498(15)	5795(3)	18(3)
C00M	1640(20)	13150(19)	5452(3)	32(4)
C1	2900(16)	1290(15)	7582(3)	18(3)
C2	6541(18)	4374(16)	5888(3)	25(3)

Table S10. Fractional Atomic Coordinates (× 10^4) and Equivalent Isotropic Displacement Parameters (Å^2 × 10^3) for 2*S*. U_{eq} is defined as 1/3 of the trace of the orthogonalised U_{IJ} tensor.

Atom	*x*	*y*	*z*	*U(eq)*
Pb01	2601.9(8)	9177.8(7)	3275.4(2)	36.0(2)
Pb02	-2366.2(8)	4212.8(8)	3257.0(2)	38.6(2)
Br03	3027(3)	8517(2)	3973.9(5)	62.7(6)
Br04	4866(3)	6498(3)	3171.9(6)	62.8(6)
Br05	-3038(3)	4606(3)	3928.1(5)	64.2(6)
Br06	5268(3)	11488(3)	3314.4(8)	70.2(7)
Br07	2705(4)	9453(3)	2529.4(5)	72.0(7)
Br08	471(3)	2067(3)	3371.8(8)	79.8(8)

Atom	*x*	*y*	*z*	*U*(*eq*)
Br09	-166(3)	6909(3)	3321.1(8)	73.5(8)
Br00	4734(7)	2837(7)	4818.6(10)	160(2)
Br1	-2112(13)	7089(10)	5044(2)	280(6)
N00C	2890(20)	4660(20)	3825(4)	58(4)
N00D	-2900(30)	8580(30)	3858(5)	86(7)
C00E	3050(30)	2540(20)	4215(5)	65(6)
C00F	3100(40)	1910(30)	4555(6)	95(9)
C00G	-1860(50)	8950(40)	4141(8)	130(9)
C14	2740(30)	4260(20)	4182(5)	54(5)
C22	1080(30)	4690(30)	4298(7)	77(7)
C24	-1800(60)	10670(40)	4169(10)	141(12)
C2	-2610(50)	8280(60)	4449(9)	147(9)
C1	-1390(50)	8510(50)	4714(9)	161(11)
N1	3480(30)	13290(30)	2614(8)	103(9)
C3	1910(60)	15420(50)	2448(12)	170(20)
C4	1880(40)	13720(50)	2492(14)	180(20)

Table S11. Selected bond lengths (Å) for 2*R*.

Atom-Atom	Length (Å)	Atom-Atom	Length (Å)
Pb01-Br04	2.8140(12)	Br0A-C00G	1.945(12)
Pb01-Br05[1]	3.0808(12)	Br0B-C00M	1.968(16)
Pb01-Br06	2.9609(13)	N00C-C00K	1.514(15)
Pb01-Br07	3.0059(12)	N00D-C1	1.509(16)
Pb01-Br08[2]	3.2135(12)	C00E-C00J	1.514(16)
Pb01-Br09[3]	3.0982(13)	N00F-C00J	1.504(14)
Pb02-Br03	2.9741(12)	C00G-C00I	1.510(17)
Pb02-Br05	2.9530(13)	C00H-C1	1.508(18)
Pb02-Br06	3.0306(13)	C00I-C00K	1.543(16)
Pb02-Br07[4]	3.1571(13)	C00J-C00L	1.519(17)

Pb02-Br08	3.0142(12)	C00K-C2	1.496(18)
Pb02-Br09	2.9822(13)	C00L-C00M	1.504(17)

[1]1+X,+Y,+Z; [2]1-X,1/2+Y,3/2-Z; [3]1+X,1+Y,+Z; [4]+X,-1+Y,+Z

Table S12. Selected bond lengths (Å) for 2*S*.

Atom-Atom	Length (Å)	Atom-Atom	Length (Å)
Pb01-Br03	2.928(2)	Br07-Pb02[7]	3.228(2)
Pb01-Br04	3.019(2)	Br08-Pb01[8]	3.089(2)
Pb01-Br06	3.000(2)	Br00-C00F	1.92(3)
Pb01-Br07	3.054(2)	Br1-C1	1.92(2)
Pb01-Br08[1]	3.089(2)	N00C-C14	1.50(2)
Pb01-Br09	3.043(2)	N00D-C00G	1.48(2)
Pb02-Br04[2]	3.066(2)	C00E-C00F	1.49(3)
Pb02-Br05	2.816(2)	C00E-C14	1.51(3)
Pb02-Br06[3]	3.083(2)	C00G-C24	1.48(2)
Pb02-Br07[4]	3.228(2)	C00G-C2	1.52(2)
Pb02-Br08	3.052(2)	C14-C22	1.52(3)
Pb02-Br09	2.977(2)	C2-C1	1.50(2)
Br04-Pb02[5]	3.066(2)	N1-C4	1.48(3)
Br06-Pb02[6]	3.083(2)	C3-C4	1.468(19)

[1]+X,1+Y,+Z; [2]-1+X,+Y,+Z; [3]-1+X,-1+Y,+Z; [4]-X,-1/2+Y,1/2-Z; [5]1+X,+Y,+Z; [6]1+X,1+Y,+Z; [7]-X,1/2+Y,1/2-Z; [8]+X,-1+Y,+Z

Table S13. Selected bond angles (°) for 2*R*.

Atom-Atom-Atom	Angle (°)	Atom-Atom-Atom	Angle (°)
Br04-Pb01-Br05[1]	83.04(4)	Br05-Pb02-Br09	91.88(4)
Br04-Pb01-Br06	85.91(4)	Br06-Pb02-Br07[4]	98.57(4)
Br04-Pb01-Br07	96.13(4)	Br08-Pb02-Br06	95.75(4)
Br04-Pb01-Br08[2]	159.22(4)	Br08-Pb02-Br07[4]	88.69(4)
Br04-Pb01-Br09[3]	83.98(4)	Br09-Pb02-Br06	175.05(4)
Br05[1]-Pb01-Br08[2]	76.68(3)	Br09-Pb02-Br07[4]	82.19(4)
Br05[1]-Pb01-Br09[3]	94.57(4)	Br09-Pb02-Br08	89.15(4)
Br06-Pb01-Br05[1]	87.63(4)	Pb02-Br05-Pb01[5]	160.11(5)
Br06-Pb01-Br07	86.79(4)	Pb01-Br06-Pb02	162.39(5)
Br06-Pb01-Br08[2]	97.59(4)	Pb01-Br07-Pb02[6]	152.28(5)

Br06-Pb01-Br09[3]	169.31(4)	Pb02-Br08-Pb01[7]	169.19(5)
Br07-Pb01-Br05[1]	174.40(4)	Pb02-Br09-Pb01[8]	162.02(5)
Br07-Pb01-Br08[2]	104.49(4)	C00I-C00G-Br0A	111.2(9)
Br07-Pb01-Br09[3]	90.84(4)	C00G-C00I-C00K	110.3(10)
Br09[3]-Pb01-Br08[2]	93.09(4)	C00E-C00J-C00L	115.2(11)
Br03-Pb02-Br06	83.92(4)	N00F-C00J-C00E	108.2(10)
Br03-Pb02-Br07[4]	98.43(3)	N00F-C00J-C00L	108.0(10)
Br03-Pb02-Br08	172.85(4)	N00C-C00K-C00I	108.1(10)
Br03-Pb02-Br09	91.13(4)	C2-C00K-N00C	109.0(11)
Br05-Pb02-Br03	86.96(3)	C2-C00K-C00I	114.6(10)
Br05-Pb02-Br06	87.79(4)	C00M-C00L-C00J	113.6(11)
Br05-Pb02-Br07[4]	172.03(4)	C00L-C00M-Br0B	111.0(10)
Br05-Pb02-Br08	85.89(4)	C00H-C1-N00D	110.6(10)

[1]1+X,+Y,+Z; [2]1-X,1/2+Y,3/2-Z; [3]1+X,1+Y,+Z; [4]+X,-1+Y,+Z; [5]-1+X,+Y,+Z; [6]+X,1+Y,+Z; [7]1-X,-1/2+Y,3/2-Z; [8]-1+X,-1+Y,+Z

Table S14. Selected bond angles (°) for 2*S*.

Atom-Atom-Atom	Angle (°)	Atom-Atom-Atom	Angle (°)
Br03-Pb01-Br04	84.89(7)	Br08-Pb02-Br04[2]	176.64(7)
Br03-Pb01-Br06	89.18(8)	Br08-Pb02-Br06[3]	91.90(9)
Br03-Pb01-Br07	169.00(8)	Br08-Pb02-Br07[4]	105.09(8)
Br03-Pb01-Br08[1]	95.91(8)	Br09-Pb02-Br04[2]	89.01(8)
Br03-Pb01-Br09	84.79(8)	Br09-Pb02-Br06[3]	170.45(10)
Br04-Pb01-Br07	84.37(7)	Br09-Pb02-Br07[4]	95.29(8)
Br04-Pb01-Br08[1]	176.21(9)	Br09-Pb02-Br08	88.38(9)
Br04-Pb01-Br09	90.08(8)	Pb01-Br04-Pb02[5]	162.21(10)
Br06-Pb01-Br04	92.38(8)	Pb01-Br06-Pb02[6]	169.01(11)
Br06-Pb01-Br07	88.86(8)	Pb01-Br07-Pb02[7]	169.46(11)
Br06-Pb01-Br08[1]	83.93(9)	Pb02-Br08-Pb01[8]	156.97(10)
Br06-Pb01-Br09	173.26(10)	Pb02-Br09-Pb01	165.72(11)
Br07-Pb01-Br08[1]	94.65(8)	C00F-C00E-C14	116(2)
Br09-Pb01-Br07	97.63(9)	C00E-C00F-Br00	113(2)
Br09-Pb01-Br08[1]	93.68(8)	N00D-C00G-C24	107(3)
Br04[2]-Pb02-Br06[3]	90.34(8)	N00D-C00G-C2	109(3)

Br04[2]-Pb02-Br07[4]	77.24(7)	C24-C00G-C2	109(4)
Br05-Pb02-Br04[2]	83.16(7)	N00C-C14-C00E	107.1(16)
Br05-Pb02-Br06[3]	83.58(8)	N00C-C14-C22	109.1(18)
Br05-Pb02-Br07[4]	160.23(8)	C00E-C14-C22	112(2)
Br05-Pb02-Br08	94.60(8)	C1-C2-C00G	105(3)
Br05-Pb02-Br09	86.89(8)	C2-C1-Br1	102(2)
Br06[3]-Pb02-Br07[4]	93.85(8)	C3-C4-N1	106(3)

[1]+X,1+Y,+Z; [2]-1+X,+Y,+Z; [3]-1+X,-1+Y,+Z; [4]-X,-1/2+Y,1/2-Z; [5]1+X,+Y,+Z; [6]1+X,1+Y,+Z; [7]-X,1/2+Y,1/2-Z; [8]+X,-1+Y,+Z

Table S15. Summary of the band gap and chiroptical properties (CD/gCD) of reported Compound.

Dimension	Compound	Band gap	CD (mdeg) / g_{CD}	Ref.
1D	(*R/S*)-AMEPYPb_2Br_6	E_g = 2.813 eV	g_{CD} = 0.05	1
	(*R/S*-3AD)$PbBr_3Cl·H_2O$	E_g = 3.06 eV	$g_{CD} = 5.7 \times 10^{-3}$	2
2D	(*R/S*)-3BrMBA$_2PbBr_4$	E_g = 3.09 eV	$g_{CD} = 1.08 \times 10^{-3}$	3
	(*R/S*-β-MPA) $EA_2Pb_2Br_7$	E_g = 2.75 eV	$g_{CD} = 4.6\times 10^{-4}$	4
	(*R/S*-MPEA)$_2MA_2Pb_3I_{10}$	E_g = 2.05 eV	$g_{CD} = 8\times10^{-4}$	5
	$CsPbBr_3$ NPLs (*n* = 1 ~ 3)	*n* =1, E_g = 3 eV *n* = 2, E_g = 1.9 eV -	*n*= 1, $g_{CD} = 2.30 \times 10^{-3}$ *n* = 2, $g_{CD} = 6.67 \times 10^{-4}$ *n* = 3, $g_{CD} = 7.0 \times 10^{-5}$	6
	(*R/S*)MA-PNS/PAN (*n* = 2 ~ 5)	*n* = 2, E_g ≈ 2.82 eV *n* = 3, E_g ≈ 2.70 eV *n* = 4, E_g ≈2 .61 eV -	*n* = 2, CD ≈16.5 mdeg *n* = 3, CD ≈ 6.5 mdeg *n* = 4, CD ≈ 4.5 mdeg *n* = 5, CD ≈ 0.5 mdeg	7
	(*R/S*-NEA)$_2(MA)_{n-1}Pb_nI_{3n+1}$ (*n* =1 ~ 5)	E_g ≈ 2.46 eV~2.61 eV	*n* = 1, CD ≈ 244 mdeg *n* = 2, CD ≈ 98 mdeg *n* = 3, CD ≈ 40 mdeg *n* = 4, CD ≈ 20 mdeg *n* = 5, CD＜5 mdeg	8

AMEPY = 2-aminoethyl-1-methylpyrrolidine
3AD = 3-aminopiperidine dihydrochloride
3BrMBA = 1-(3-bromphen-yl)-ethylamine
MPA = methylphenethylammonium and EA = ethylammonium
MPEA = methylphenylethylammonium; MA = methylammonium
NEA = 1-(2-naphthyl)ethylamine

Table S16. The asymmetry factor of various reported CPL detectors.

Compound	Asymmetry factor	Ref.
(*S*/*R*-PEA)PbI_3	0.08	9
(*S*-$C_5H_{14}N$)PbI_3	0.23	10
[(*R*)-β-MPA]$_2PbCl_4$	0.1	11
(*R*-BPEA)$_2PbI_4$	0.13	12
(*S*-VPEA)$_2PbI_4$	0.22	13
[(*R*)-β-MPA]$EAPbBr_4$	0.19	14
(*R*-MBA)$_2PbI_4$	0.24	15
(*S*-MBA)$_2PbI_4$	0.209	16
(*S*-2F-MBA)$_2PbI_4$	0.288	16
[(*R*)-β-MPA]$_2MAPb_2I_7$	0.2	17
(*S*-NEA)$_2MAPb_2I_7$	0.15	8
(*R* -BrBA)$_2EA_2Pb_3Br_{10}$	0.278	This work

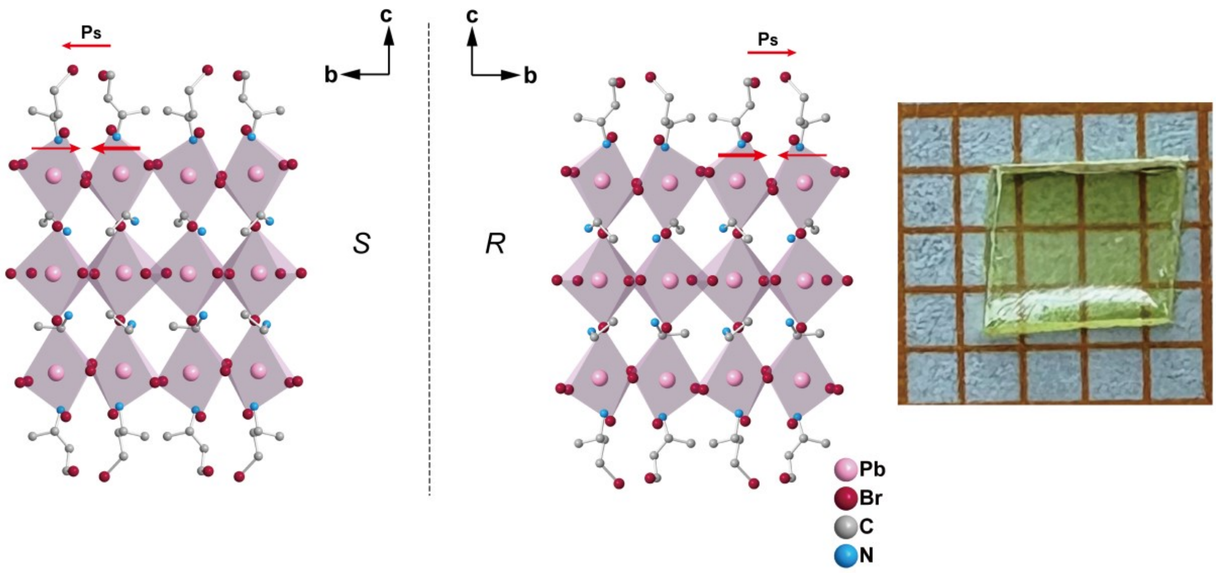

Figure S1. Chiral multilayered structures of 3*R*/*S* viewed along the *a*- axis, and the picture of crystal 3*R*. (Corresponding hydrogen atoms of organic cations are omitted for clarity.)

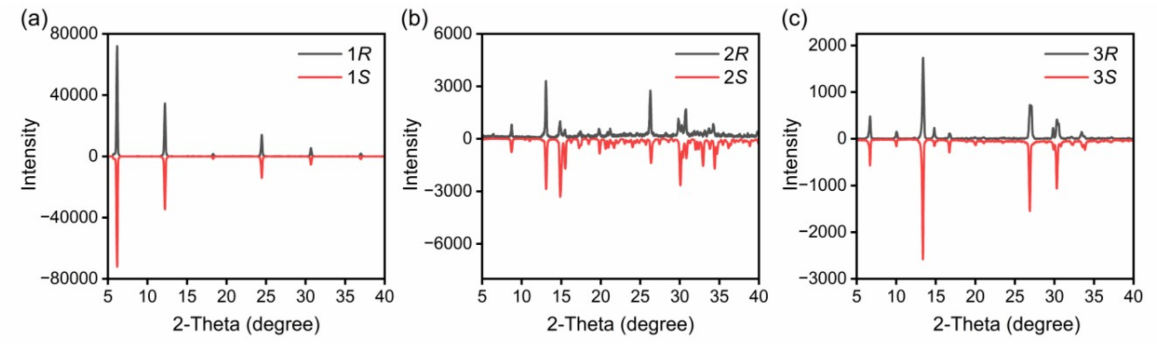

Figure S2. The powder XRD patterns of 1*R/S*,2*R/S*, and 3*R/S*.

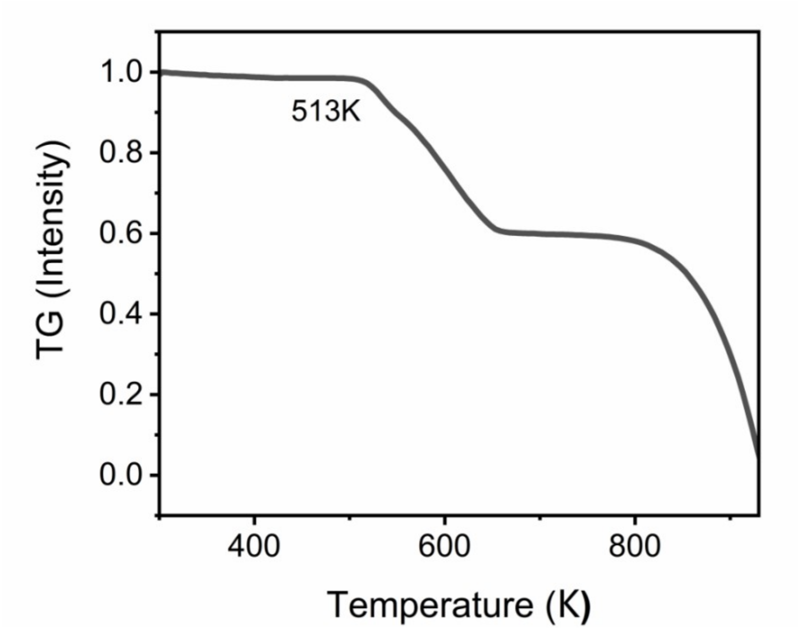

Figure S3. Thermogravimetric analysis curves for 3*R*.

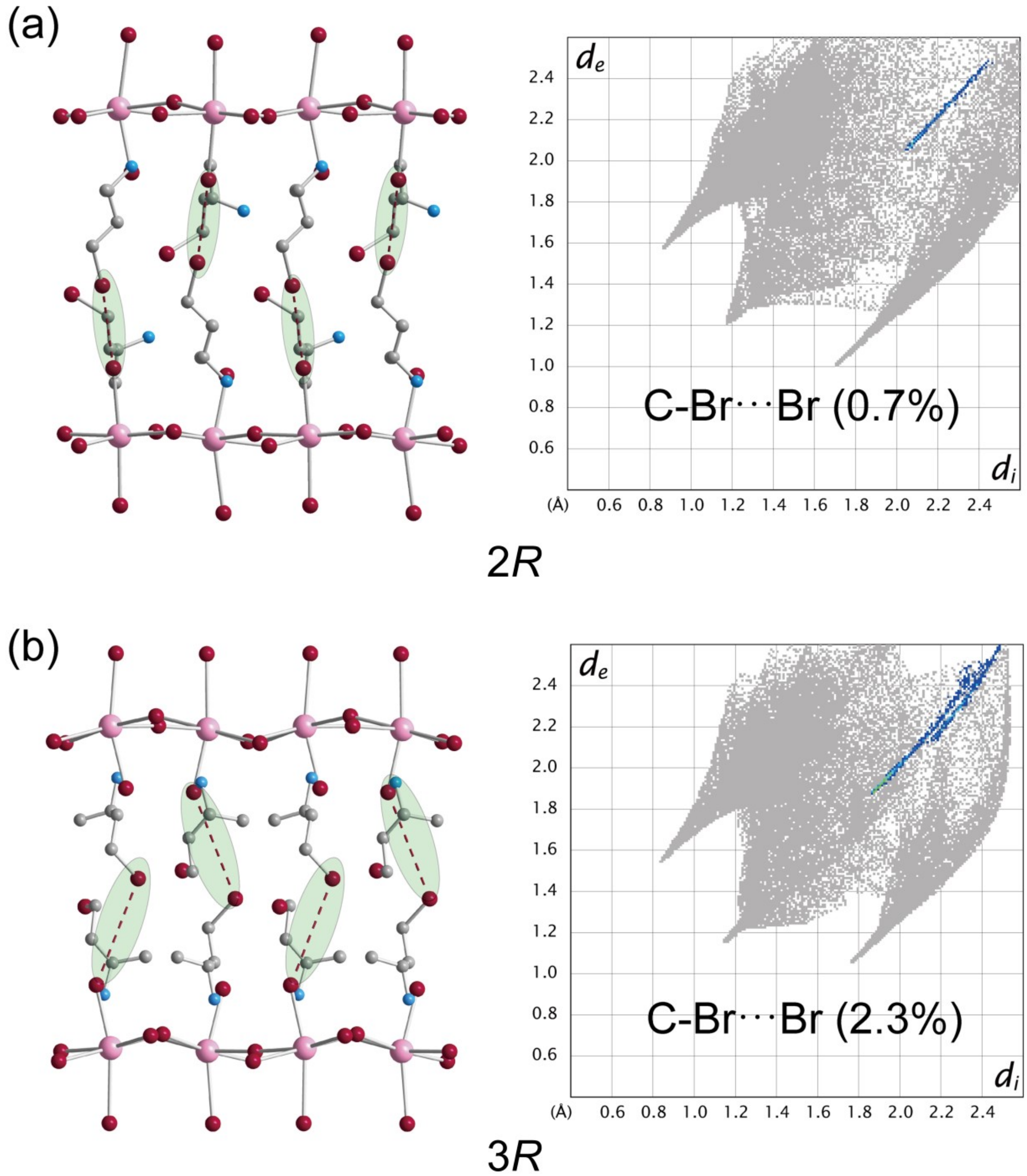

Figure S4. (a) Schematic diagram of the Br···Br bond and fingerprints expressing the strength of the Br···Br bond for 2*R*. (b)Schematic diagram of the Br···Br bond and fingerprints expressing the strength of the Br···Br bond for 3*R*.

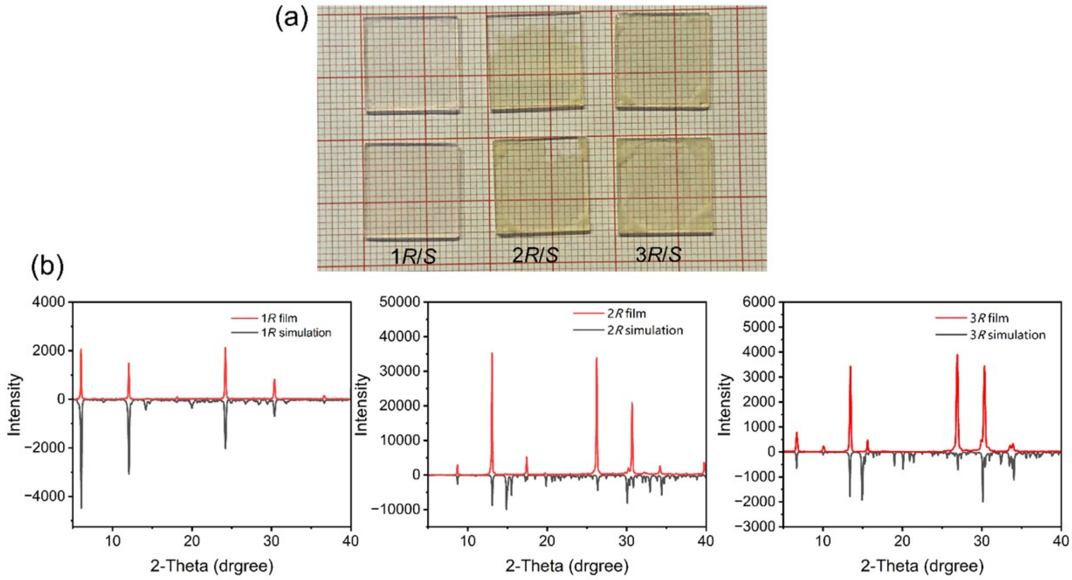

Figure S5. (a) The photo of the films for 1*R*/*S*, 2*R*/*S* and 3*R*/*S*; (b) The PXRD comparison diagram of the diaphragm of 1*R*/*S*, 2*R*/*S* and 3*R*/*S* and the theoretical simulation.

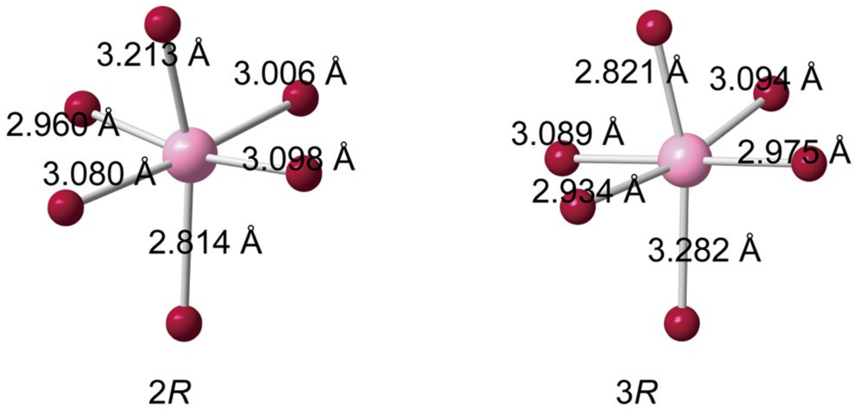

Figure S6. $[PbBr_6]^{4-}$ octahedron for 2*R* and 3*R*. Using the formula Δd_{2R} is 0.0017 and Δd_{3R} is 0.0023.

$$\Delta d = \frac{1}{6}\sum_{i=1}^{6}\left[\frac{d_i - d}{d}\right]^2$$

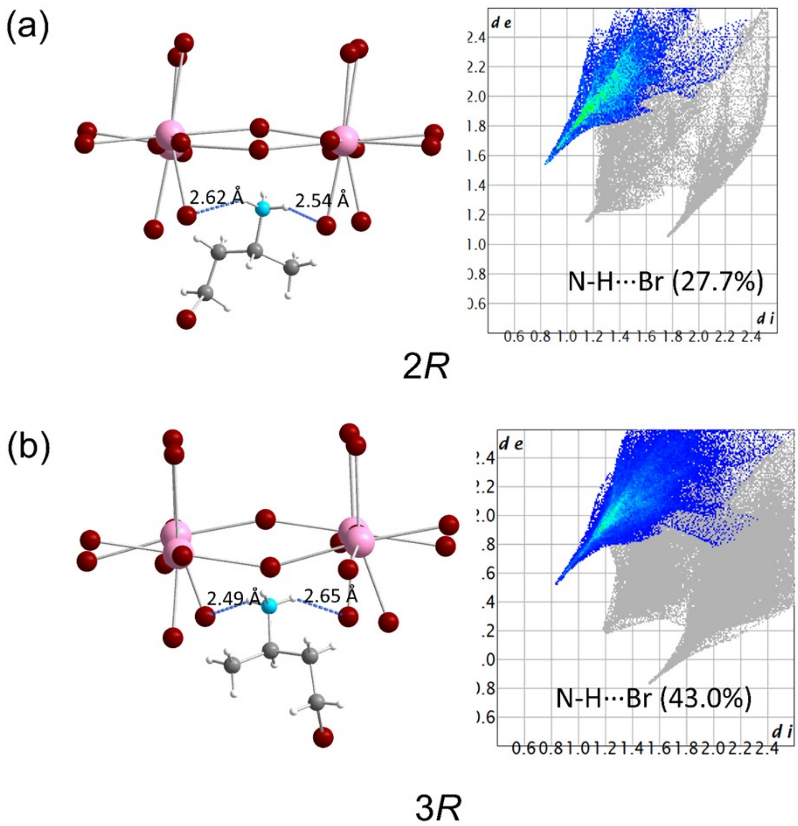

Figure S7. (a) Length of the N-H···Br bond and fingerprints expressing the strength of the N-H···Br bond for 2*R*. (b) Length of the N-H···Br bond and fingerprints expressing the strength of the N-H···Br bond for 3*R*.

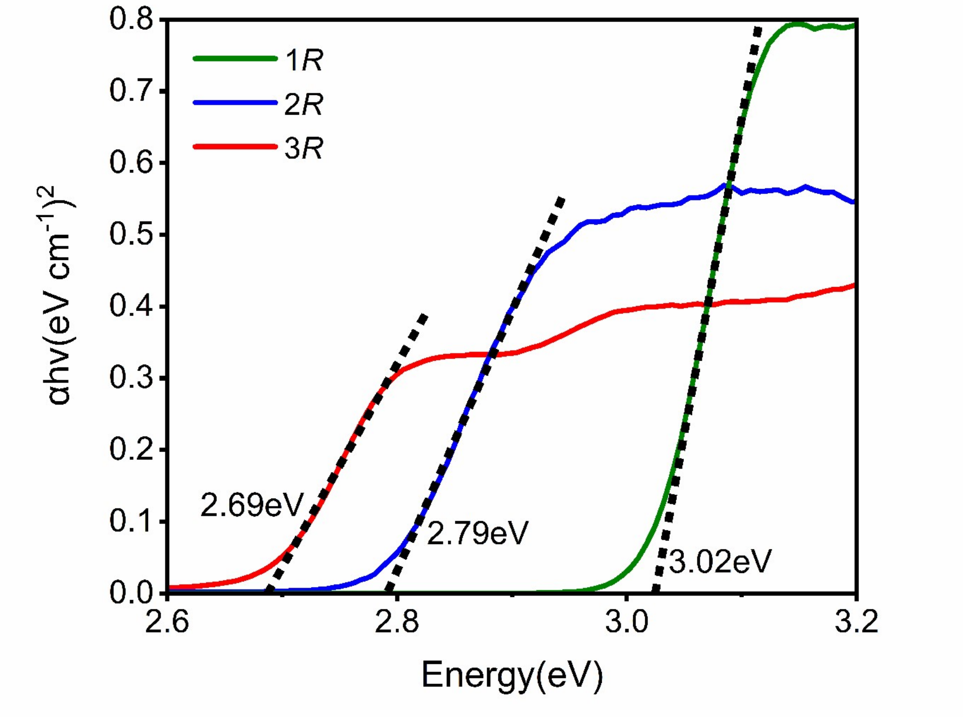

Figure S8. Bandgap calculated via Tauc for 1*R*, 2*R* and 3*R*.

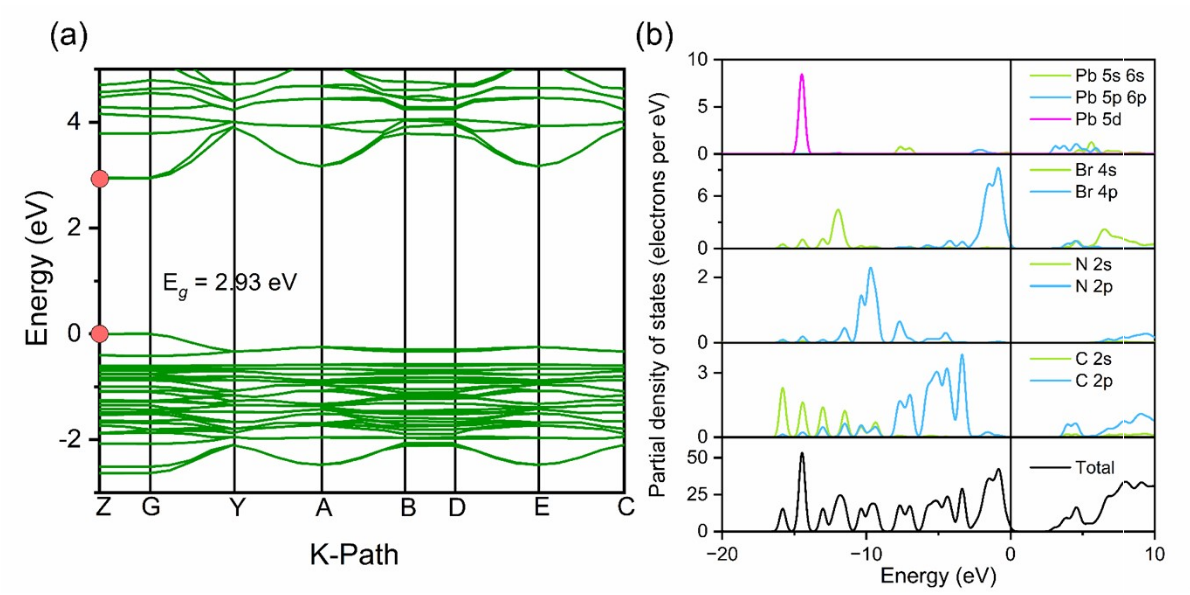

Figure S9. Calculated electronic band structures (a) and partial DOS (b) of 1*R*.

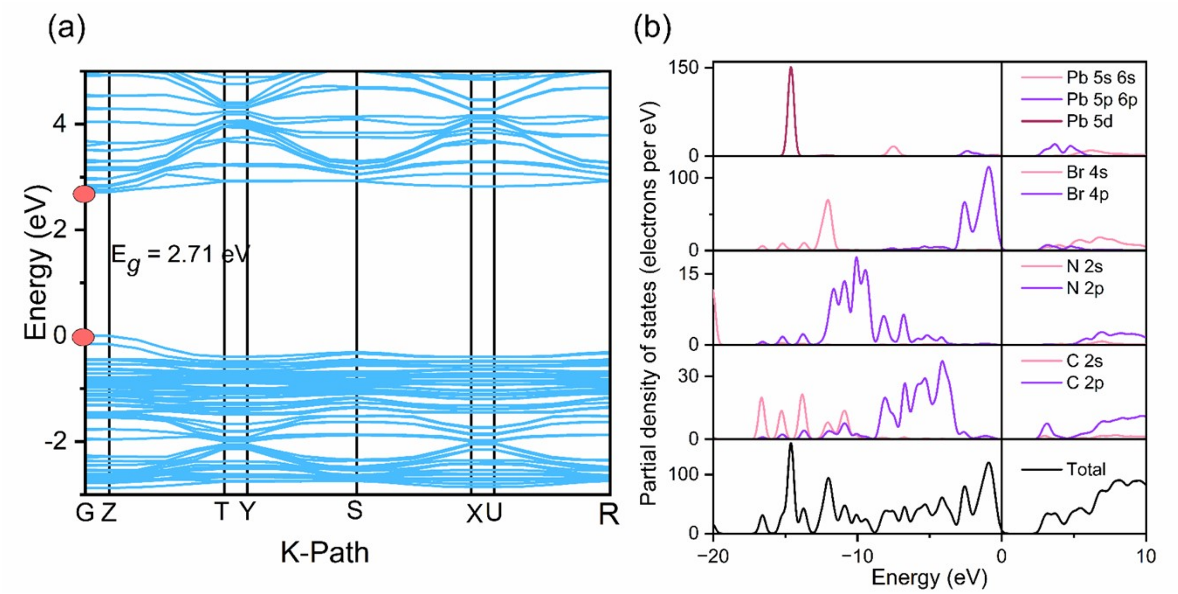

Figure S10. Calculated electronic band structures (a) and partial DOS (b) of 2*R*.

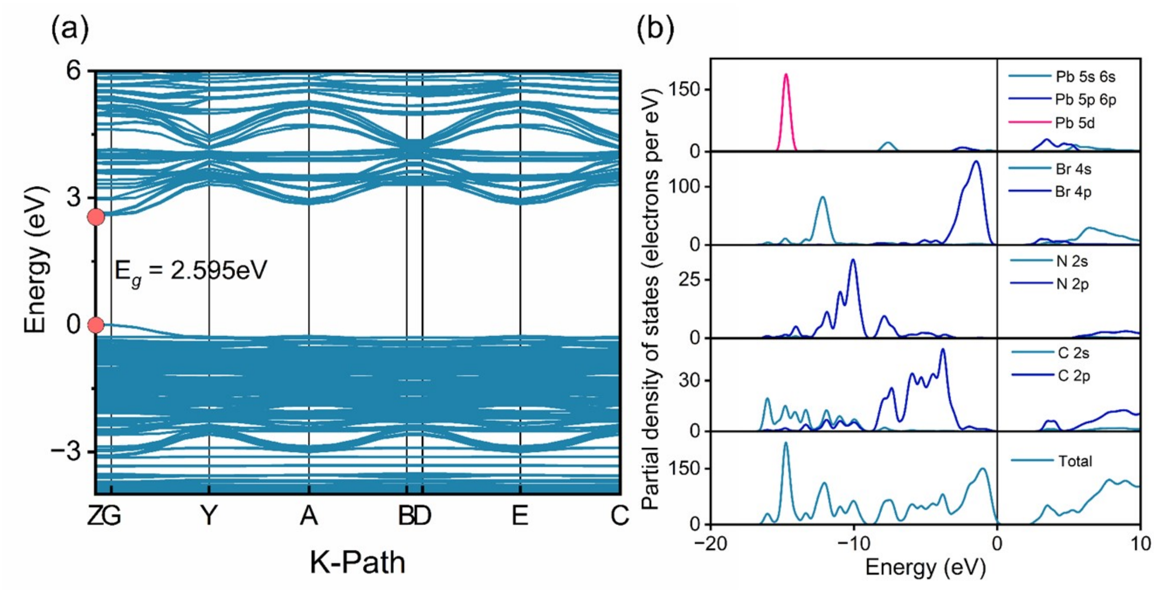

Figure S11. Calculated electronic band structures (a) and partial DOS (b) of 3*R*.

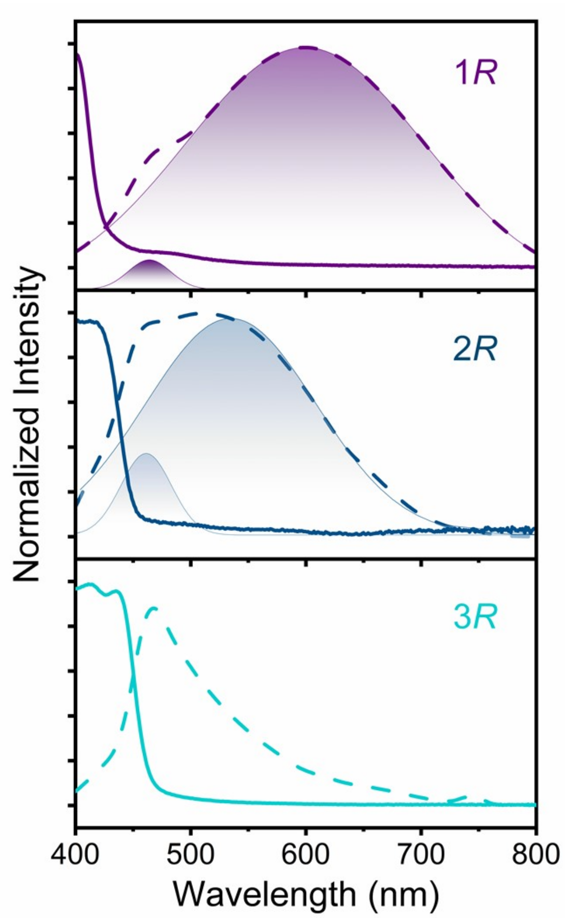

Figure S12. Absorption spectra (solid lines) and PL spectra (dashed lines) for 1R, 2R, and 3R. The PL spectra (dashed lines) are deconvoluted into multiple Gaussian components (filled colored areas)

For RP-phase perovskites with *n* = 1 (1*R*), the inorganic layers are completely isolated by organic cations, forming a highly confined two-dimensional structure that results in exciton binding energies significantly higher than room-temperature thermal kinetic energy. The lattice's "softness" and anisotropy markedly enhance exciton-phonon coupling, where exciton-lattice interactions induce localized lattice distortions leading to self-trapped excitons (STE). Consequently, 1*R* samples exhibit luminescence behavior dominated by STE recombination, characterized by broad emission peaks (half-width at half maximum>100 nm) and substantial Stokes shifts corresponding to the low-energy broad peak at 590 nm in the photoluminescence spectrum. Concurrently, weak free exciton (FE) emission is detectable at 462 nm. When the number of layers increases to *n* = 2 (2*R*), the inorganic layer thickness increases, the quantum confinement effect weakens, the exciton binding energy decreases, lattice rigidity strengthens, and the exciton-phonon coupling strength diminishes, leading to reduced stability of STE. Consequently, 2*R* samples exhibit a transition from STE to band-edge FE emission: a distinct FE emission peak appears at

464 nm, while a STE broad peak persists at 530 nm. For samples with n = 3 (3*R*), the quantum confinement effect further diminishes, with the electronic structure approaching that of three-dimensional perovskites. The exciton binding energy decreases, and lattice rigidity increases significantly, effectively suppressing the formation of self-bound states. At this stage, the luminescence mechanism is predominantly driven by band-edge FE recombination, exhibiting a sharp, narrow linewidth emission peak at 469 nm in the spectrum, while no distinct STE emission signals are observed in the low-energy region.

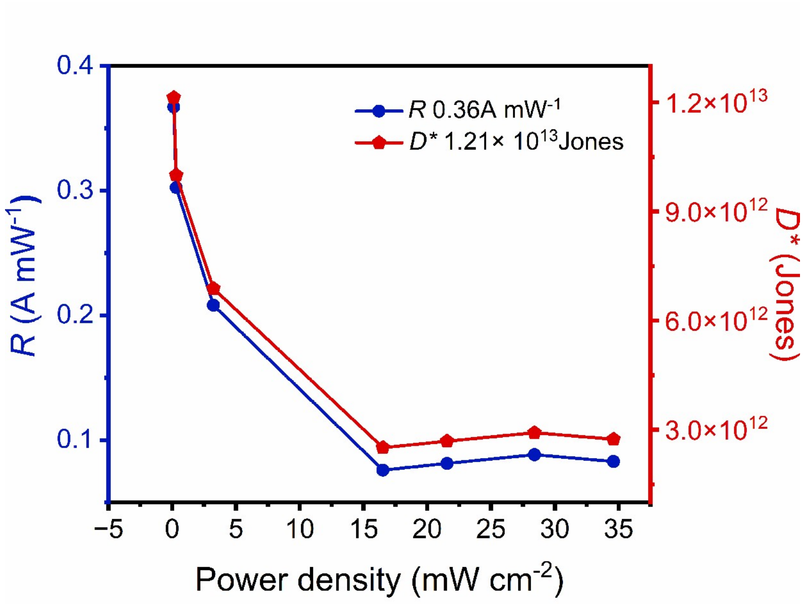

Figure S13. The responsivity (*R*) and detectivity (*D**) of the 3*R* device.

$$R = \frac{I_{photo} - I_{dark}}{PS}$$

$$D^* = \frac{R}{\sqrt{2qI_{dark}/S}}$$

where I_{photo}, I_{dark}, P, S, and q represent the photocurrent, dark current, light power density, effective area, and charge constant, respectively.

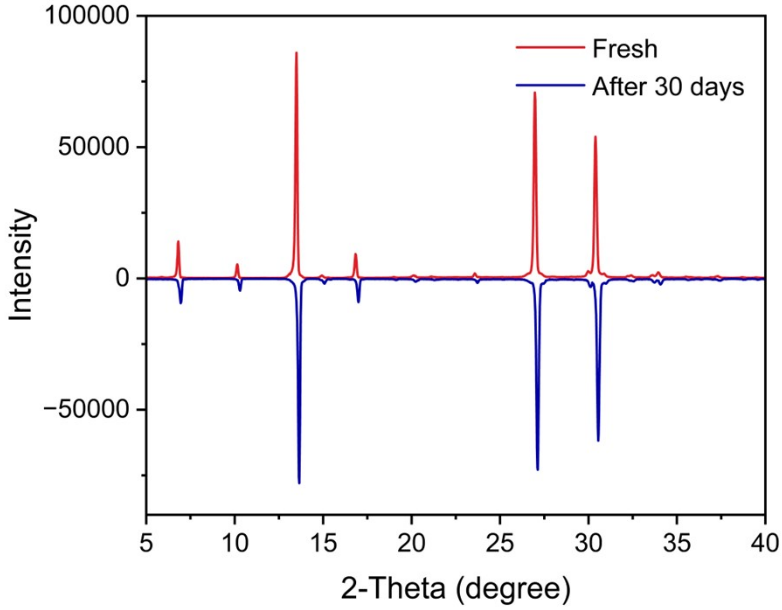

Figure S14. The XRD of 3*R* was measured on the fresh powder and after 30 days.

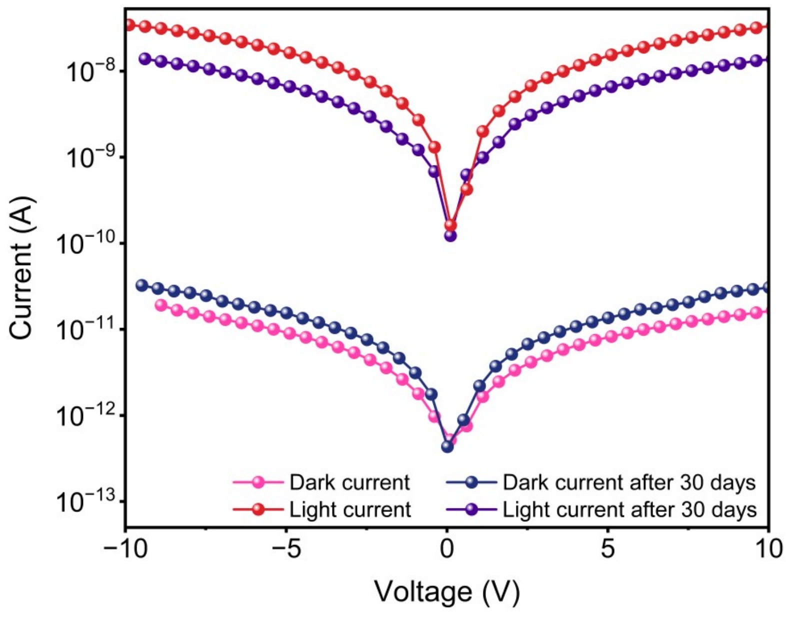

Figure S15. The I-V curves of 3*R* were measured on the fresh sample and after 30 days.

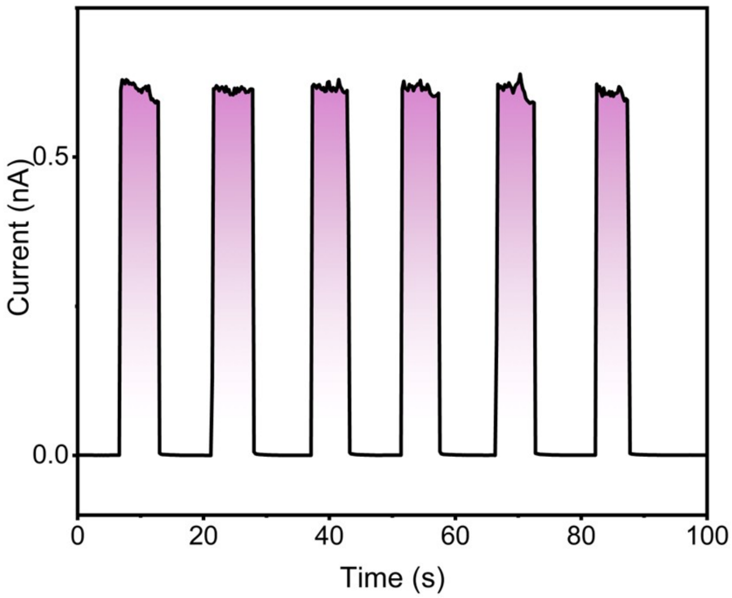

Figure S16. The real-time-dependent reproducible photovoltage for 3*R*.

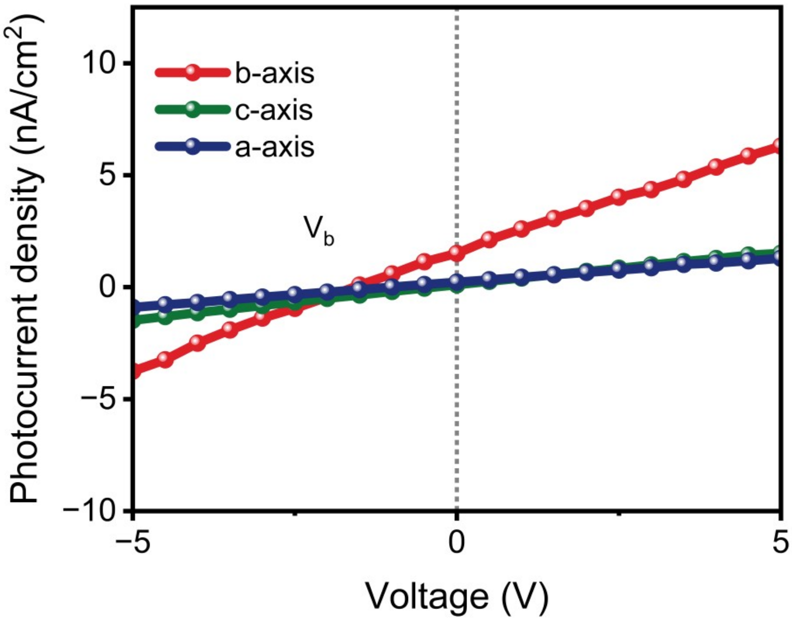

Figure S17. The intrinsic bulk photovoltaic effect measured along the *b*-axis for 3*R*.

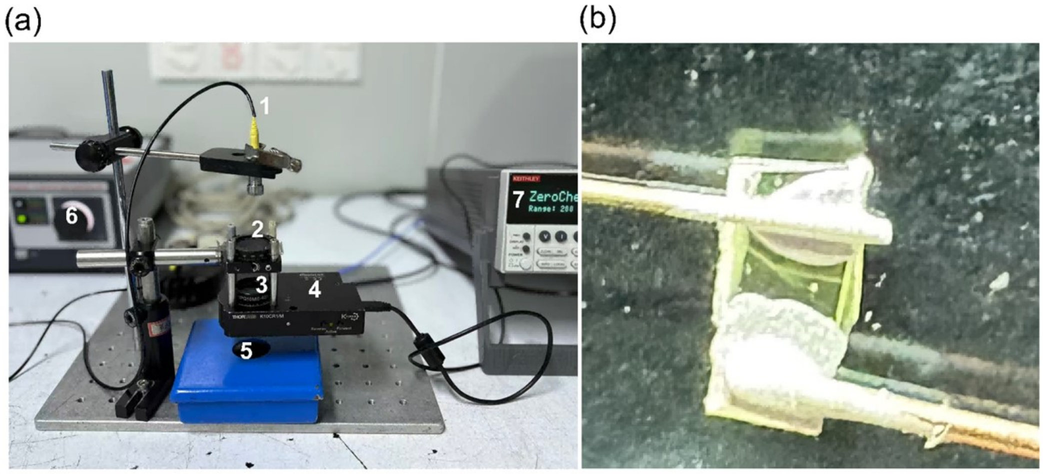

Figure S18. The photos of the single-crystal sample and the device for the CPL detection.

1: Fiber output laser head (Thorlabs LP405-MF300,405 nm)

2: Optical lens

3: 405 nm fiber collimator (Thorlabs MPQ10ME-405)

4: Electric rotary stage (Thorlabs K10CR1/M)

5: Electrode box with built-in single-crystal electrode

6: Desktop laser diode driver/TEC controller (ITC40017)

7: Electrostatic meter (Model 6517B)

References.

1 H. Zheng, Z. Wu, J. Shao, J. Lan, Y. Liu, H. Xiong, J. Fan and W. Li, *Adv. Funct. Mater.*, 2025, e13402.

2 M. Su, X. Wu, J. Zhang, M. Wang, J. Ma, L. Lian, C. Dun, Q. Zeng, Q. Liu, Y. Tian, X. Chen, M. Jia, Y. Liu, Y. Han, Z. Ma, D. Wu, X. Li and Z. Shi, *Small Methods*, 2026, **10**, e02219.

3 D. Hu, Z. Zhang, K. Zhang, Q. He and W. Zhao, *J. Semicond.*, 2025, **46**, 72102.

4 W. Wu, X. Shang, Z. Xu, H. Ye, Y. Yao, X. Chen, M. Hong, J. Luo and L. Li, *Adv. Sci.*, 2023, **10**, 2206070.

5 S. Ramakrishnan, Y. Dong, Y. Xie, J. L. Shelton, M. P. Hautzinger, D. Nguyen Minh, M. Taddei, X. Zhang, Y. Zhang, D. B. Mitzi, M. A. Haque, J. L. Blackburn, Q. Yu, M. C. Beard and J. M. Luther, *J. Am. Chem. Soc.*, 2025, **147**, 44457–44467.

6 Q. Cao, R. Song, C. C. S. Chan, Z. Wang, P. Y. Wong, K. S. Wong, V. Blum and H. Lu, *Adv. Opt. Mater.*, 2023, **11**, 2203125.

7 Z. Wen, R. Lu, F. Gu, K. Zheng, L. Zhang, H. Jin, Y. Chen, S. Wang and S. Pan, *Adv. Funct. Mater.*, 2023, **33**, 2212095.

8 T. Liu, W. Shi, W. Tang, Z. Liu, B. C. Schroeder, O. Fenwick and M. J. Fuchter, *ACS Nano*, 2022, **16**, 2682–2689.

9 C. Chen, L. Gao, W. Gao, C. Ge, X. Du, Z. Li, Y. Yang, G. Niu and J. Tang, *Nat. Commun.*, 2019, **10**, 1927.

10 Y. Zhao, X. Li, J. Feng, J. Zhao, Y. Guo, M. Yuan, G. Chen, H. Gao, L. Jiang and Y. Wu, *Giant*, 2022, **9**, 100086.

11 X. Zhang, W. Weng, L. Li, H. Wu, Y. Yao, Z. Wang, X. Liu, W. Lin and J. Luo, *Small*, 2021, **17**, 2102884.

12 Y. Qin, F.-F. Gao, S. Qian, T.-M. Guo, Y.-J. Gong, Z.-G. Li, G.-D. Su, Y. Gao, W. Li, C. Jiang, P. Lu and X.-H. Bu, *ACS Nano*, 2022, **16**, 3221–3230.

13 Y. Zhao, X. Yin, Z. Gu, M. Yuan, J. Ma, T. Li, L. Jiang, Y. Wu and Y. Song, *Adv. Funct. Mater.*, 2023, **33**, 2306199.

14 W. Wu, X. Shang, Z. Xu, H. Ye, Y. Yao, X. Chen, M. Hong, J. Luo and L. Li, *Adv. Sci.*, 2023, **10**, 2206070.

15 Z. Liu, C. Zhang, X. Liu, A. Ren, Z. Zhou, C. Qiao, Y. Guan, Y. Fan, F. Hu and Y. S. Zhao, *Adv. Sci.*, 2021, **8**, 2102065.

16 J. Son, G. Jang, S. Ma, H. Lee, C. U. Lee, S. Yang, J. Lee, S. Moon, W. Jeong, J. H. Park, J. Kim, D. H. Kim, J. Park and J. Moon, *Adv. Funct. Mater.*, 2025, **35**, 2413041.

17 L. Wang, Y. Xue, M. Cui, Y. Huang, H. Xu, C. Qin, J. Yang, H. Dai and M. Yuan, *Angew. Chem. - Int. Ed.*, 2020, **59**, 6442–6450.